

## Research Article

# Adsorption Studies on the Removal of Textile Effluent over Two Natural Eco-Friendly Adsorbents

Ouissal Assila,<sup>1</sup> Karim Tanji ,<sup>1</sup> Morad Zouheir,<sup>1</sup> Abdellah Arrahli ,<sup>2</sup> Loubna Nahali,<sup>1</sup> Farid Zerrouq,<sup>1</sup> and Abdelhak Kherbeche<sup>1</sup>

<sup>1</sup>Laboratory of Catalysis, Materials and Environment, Higher School of Technology, Sidi Mohamed Ben Abdellah University of Fez, 30000 Fez, Morocco

<sup>2</sup>Euromed Research Center, National Institute of Applied Sciences, Euro-Mediterranean University of Fez, Morocco

Correspondence should be addressed to Karim Tanji; karimtanji1992@gmail.com

Received 24 April 2020; Revised 15 June 2020; Accepted 17 June 2020; Published 13 August 2020

Academic Editor: Pedro Avila Pérez

Copyright © 2020 Ouissal Assila et al. This is an open access article distributed under the Creative Commons Attribution License, which permits unrestricted use, distribution, and reproduction in any medium, provided the original work is properly cited.

This study investigates the possibility of applying an adsorption process using two abundant natural minerals M1 and M2. Without pretreatment or activation, the adsorbents were used to treat real textile wastewater samples (collected from Fez city, Morocco). As a cost-effective alternative, these materials were characterized by different analyses, including X-ray diffraction (XRD), scanning electron microscopy (SEM), Fourier transform infrared spectroscopy (FTIR), and X-ray fluorescence (XRF). Chemical oxygen demand (COD) and biological oxygen demand (BOD) were used to characterize the textile wastewater. Additionally, the influence of operating conditions (contact time, adsorbent dosages, and pH) was evaluated. Results show that the adsorption process takes place quickly, reaching the equilibrium at 90 and 160 min for M1 (88% COD) and M2 (79% COD). Both materials show a higher affinity to Cr (39%) and lower affinity to Cu (28%). A pseudo-second-order kinetic model provides the best fit to the experimental adsorption data. Germination tests indicate a low toxicity after the adsorption process. Performance of both materials was compared with that of other literature studies.

## 1. Introduction

Water is the source of life on Earth. However, various human activities, such as industrial, domestic usage, or agricultural, cause its pollution. For instance, there are still significant quantities of dyes in wastewater coming from textile, tannery industry, sugarcane industry, and dyeing industries [1, 2]. The release of these effluents causes an abnormal coloration of the surface waters. Some researchers determined that textile wastewaters are considered to be the most polluted water because of the presence of a high amount of dyes which have a toxic effect on the environment [3], due to dyes, pH changing, biological oxygen demand (BOD), chemical oxygen demand (COD), the presence of a large quantity of suspended solids, total dissolved solids (TDS), and salts and organic compounds [4–7]. Thus, legislations controlling the use of these substances have been established in many countries. However, in various developed countries, due to the lack of water, there is a great

necessity for recycling and reusing wastewater for industrial and agricultural purposes. Consequently, the textile and dyeing industry has begun seeking efficient methods for the removal of dyes. Meanwhile, there are various treatment processes that have been investigated and employed extensively for dyes elimination from wastewater [8, 9], including coagulation and flocculation [10], biological treatment using anaerobic granular [11], catalytic wet oxidation photochemical treatment [12–14], Fenton's process, and adsorption technology. However, many of these technologies are expensive and complex when used to treat these dyes. Consequently, the adsorption technique seems to have the best potential for wastewater treatment in industry [15], thanks to its great capacity to purify contaminated water and economic aspects [2].

The aim of this study is to investigate the possibility of using two abundant natural mineral materials (collected from two Moroccan regions) as adsorbents to treat real textile wastewater (Fez city, Essabbaghine). The investigation

will focus on using the materials without pretreatment or activation to reveal their cost effectiveness compared to other treated adsorbents from the literature and to prove their eco-friendly processes. In order to accomplish this examination, physicochemical characteristics of the textile wastewater (COD, BOD, etc.) and characterization of the two natural adsorbents were highlighted. Also process key parameters optimization (adsorbent dose, contact time, dilution factor, and temperature), isotherms, kinetics, toxicity, and desorption studies are important for both adsorbents to prove their effectiveness.

## 2. Materials and Methods

**2.1. Adsorbents Preparation.** The natural mineral materials M1 and M2 used in this study were collected from the regions of Berrechid and Tiflet, respectively (Morocco) (Figure 1). The natural materials were primarily washed several times by distilled water and dried for 24 h at 100°C then milled and sieved, acquiring the average diameter of 80  $\mu\text{m}$ . During the adsorption experiment, HCl (0.5 M) and NaOH (0.5 M) from Sigma-Aldrich were used to adjust the pH solution without further purification.

**2.2. Adsorption Experiments.** The adsorption over M1 and M2 test was carried out by using a mass of adsorbent mixed with a solution of textile wastewater at room temperature under continuous stirring. In order to investigate the kinetic of the adsorption, a 5 ml sample was collected each 10 min to measure its concentration. The adsorption efficiencies were calculated using formula (1) [16, 17], where  $C_0$  and  $C_t$  are, respectively, the initial and the final COD concentrations ( $\text{mgO}_2\cdot\text{L}^{-1}$ ). COD was determined from the closed reflux tube method (5220D). Two equations were used to investigate the kinetic studies, number (2) for pseudo-first-order (PFO) and (3) for pseudo-second-order (PSO) [18, 19]. The Langmuir isotherm admits that adsorptions happen at specific homogeneous active sites on the adsorbent surface; (4) is its corresponding equation, where  $K_L$  is the Langmuir constant ( $\text{L}\cdot\text{mg}^{-1}$ ) [20]. The Freundlich model describes the nonuniform and multilayer adsorption on heterogeneous surfaces; its model is represented by equation (5), where  $K_F$  is the adsorption capacity and  $1/n$  represents the intensity of adsorption. The germination rate was calculated using (6) as reported in [21, 22].

$$\text{adsorption (\%)} = \frac{(C_0 - C_t)}{C_0} \times 100, \quad (1)$$

$$\ln(q_e - q_t) = \ln q_e - k_1 t, \quad (2)$$

$$\frac{t}{qt} = \frac{1}{k_2 q_e^2} + \frac{t}{q_e}, \quad (3)$$

$$\frac{C_e}{q_e} = \frac{C_e}{q_m} + \frac{1}{K_L \cdot q_m}, \quad (4)$$

$$\log q_e = \log K_F + \frac{1}{n} \log C_e, \quad (5)$$

$$\text{germination rate \%} = \frac{\% \text{ of germination blank} - \% \text{ of germination test}}{\% \text{ of germination test}}. \quad (6)$$

**2.3. Characterization Techniques.** The X-ray diffraction (X'PERT PRO) equipped with a detector operating at 40 KV and 30 mA with Cu  $K\alpha$  radiation ( $\lambda = 1.540598 \text{ \AA}$ ). Infrared spectroscopy (VERTEX 70) and scanning electron microscopy (QUANTA 200) were used to identify the composition and the morphology of adsorbents materials. The X-ray fluorescence (XRF) was used to explore the chemical composition of M1 and M2.

## 3. Results and Discussion

**3.1. Effluent Characteristics.** The solution of the studied wastewater has a violet color, a sign of the presence of a significant load of dyes and suspended solids (MES). Table 1 shows that the effluent has a pH of about 6.2 and therefore

does not require any neutralization. A conductivity of around  $252 \mu\text{s}\cdot\text{cm}^{-1}$  at 22°C, explained by the low presence of ions. Likewise, the effluent has a very low value of biological oxygen demand ( $\text{BOD}_5$ ) which is equal to  $20 \text{ mg}\cdot\text{L}^{-1}$  and a chemical oxygen demand (COD) of  $440 \text{ mg}\cdot\text{L}^{-1}$ . The values of these two parameters indicate that the effluent is not too loaded with organic and mineral matter [23].

The precipitation test was carried out during 48 hours at room temperature. The result (Figure 2) shows that turbidity decreases from 125 to 13 NTU.

**3.2. Adsorbents Characterization.** The XRD diffractograms (Figure 3) of the two sieved adsorbents indicate a distinguished mineralogical composition. We note the presence of

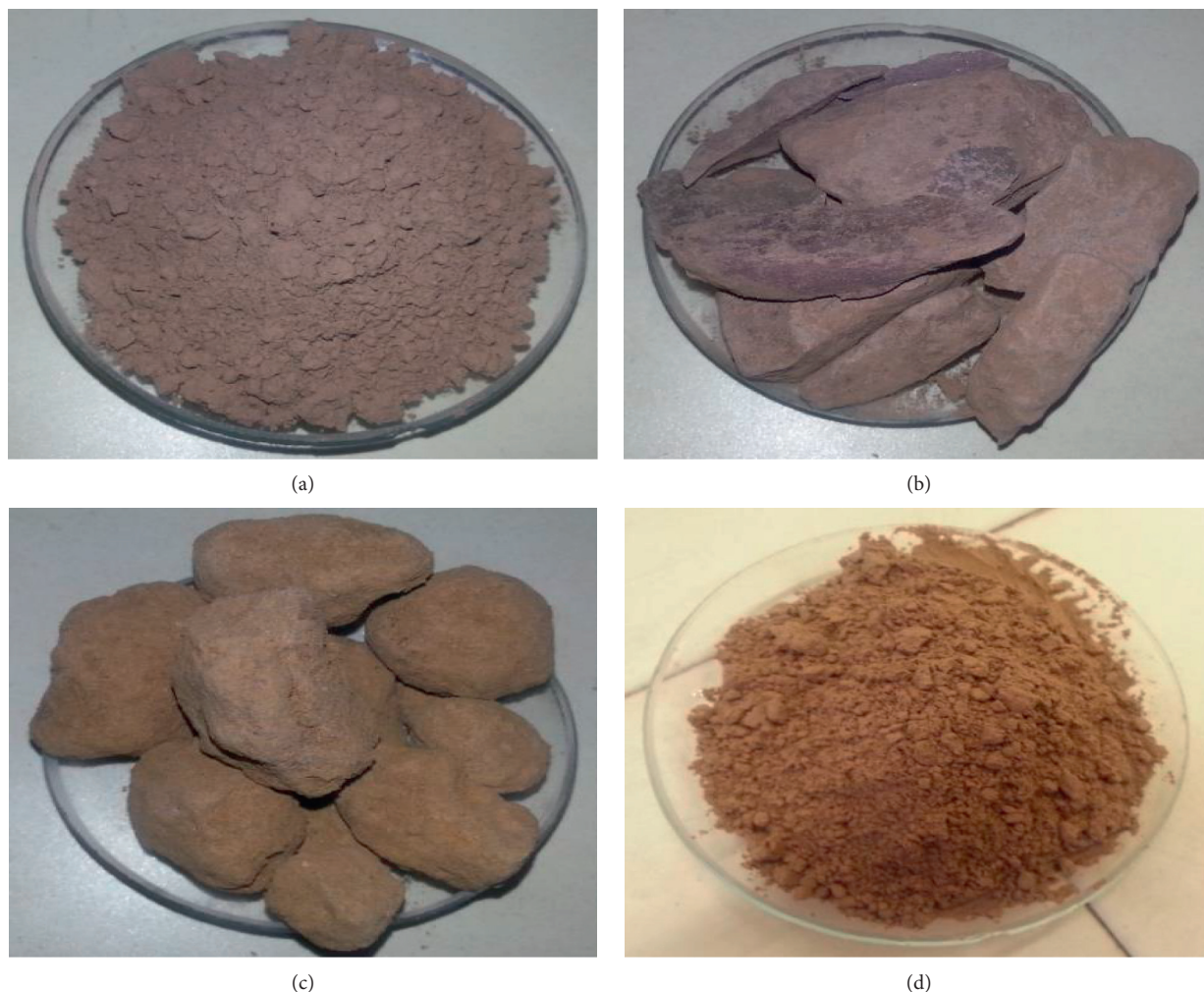


FIGURE 1: Natural raw material adsorbents M1 (a, b) and M2 (c, d).

TABLE 1: Physicochemical characteristics of the textile wastewater.

Parameters	Textile wastewater	Moroccan standards [23]
Temperature (°C)	22.7 ± 1	30
pH	6.2 ± 0.5	5.5–9.5
Color	Purple	–
MES (mg·L <sup>-1</sup> )	3016	100
Conductivity (μs·cm <sup>-1</sup> )	252	2700
Turbidity (NTU)	125	–
COD (mg O <sub>2</sub> ·L <sup>-1</sup> )	440	500
BOD <sub>5</sub> (mg O <sub>2</sub> ·L <sup>-1</sup> )	20	100
Ca (mg·L <sup>-1</sup> )	0.04	0.25
Cr (mg·L <sup>-1</sup> )	0.24	2
Cu (mg·L <sup>-1</sup> )	0.14	2
Fe (mg·L <sup>-1</sup> )	1	5
Zn (mg·L <sup>-1</sup> )	1.29	5
As (mg·L <sup>-1</sup> )	<0.01	0.1
Pb (mg·L <sup>-1</sup> )	<0.01	1
Ni (mg·L <sup>-1</sup> )	<0.01	5

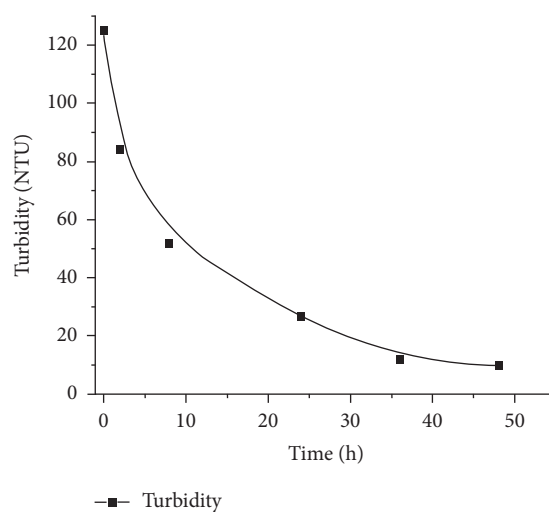


FIGURE 2: Turbidity of textile dyes from Fez city.

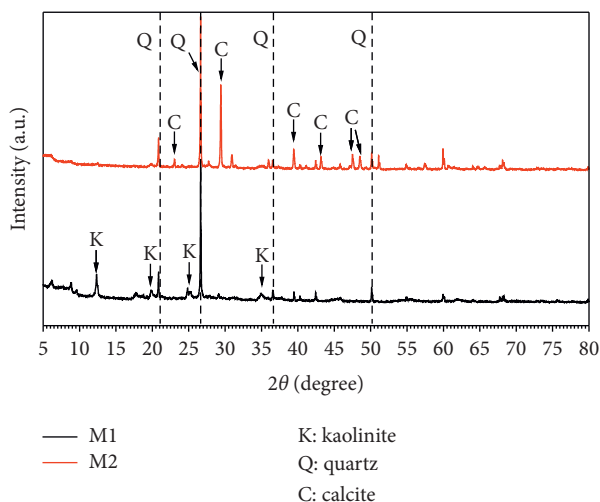


FIGURE 3: X-ray diffraction of M1 and M2 adsorbents.

quartz phase at  $2\theta$  equal to 20.9, 26.6, 29.3, and 36.4 JCPDS no. 00-046-1045 as well as the presence of the characteristic peaks of kaolinite phase at 12.34, 20.00, 26.62, and 35.00 JCPDS no. 00-029-1488 in the material of the Berrechid region M1 [24, 25]. On the other hand, Tiflet sample (M2) is distinguished by a strong presence of two phases which are quartz JCPDS no. 00-046-1045 and calcite at 23.2, 29.5, and 43.1 reported as JCPDS no. 01-086-2334 [26].

The analysis of the X-ray fluorescence (XRF) results obtained for the fractions of the two adsorbents with a diameter of less than  $80\ \mu\text{m}$  indicates that the predominant oxide for the two samples is silica (53%) followed by an abundant amount of alumina  $\text{Al}_2\text{O}_3$  (26%) and iron oxide  $\text{Fe}_2\text{O}_3$  (5.61%); the phase of iron does not appear in the XRD diffractograms, which may be due to its presence in an amorphous state. Sample M2 contains a high CaO content (18.8%) indicating the abundance of calcite. Losses on fire are of the order of 6.58% for M1 and 18.7% for M2; the latter is high due to its calcium nature (Table 2). The contents of alkaline and alkaline Earth oxides ( $\text{Na}_2\text{O}$ ,  $\text{K}_2\text{O}$ ,  $\text{MgO}$ , and  $\text{CaO}$ ) are presented in a small percentage.

FTIR spectra of the two materials M1 (Figure 4(a)) and M2 (Figure 4(b)) reveal absorption bands in the  $4000\text{--}400\ \text{cm}^{-1}$  range corresponding to different functional groupings (Figure 4) of the M2 sample which shows relatively the same band found in the M1 spectrum at  $3620$ ,  $3436$  and at  $1628\ \text{cm}^{-1}$  corresponding to the O-H stretching vibrations [27, 28]. For the intense bands coming out at  $1419$  and at  $714\ \text{cm}^{-1}$ , characteristics of the carbonates are attributed to the calcite which is more abundant [29]. The other bands at  $1024$  and  $519\ \text{cm}^{-1}$  correspond to Si-O-Si and Si-O-Al, respectively, which matches perfectly with the XRD results [30, 31].

Figure 5 illustrates the scanning electron microscopy (SEM) to observe the morphology of both adsorbents. Figures 5(a) and 5(b) show M1 in different magnifications which are found to be more porous and homogeneous on the surface more than M2 (Figures 5(c) and 5(d)) which seems to be grainier with homogeneous agglomerated particles.

The interstice diameter varies between 6 and  $11\ \mu\text{m}$  for M1 and between 2 and  $5\ \mu\text{m}$  for M2. This can explain the adsorption performance of M1 as it presents more surface area than M2, which is clearly shown in these images.

**3.3. Adsorption of Textile Dyes.** In order to study the adsorption of textile wastewater over M1 and M2, the effects of various parameters on the adsorption efficiency were investigated in this section.

The effect of the contact time on the absorption rate was studied by putting 1 g of adsorbents in one liter of the textile wastewater solution diluted 10 times (pH 2) at room temperature. The obtained results (Figure 6) show that the adsorption of the effluent on the two adsorbents M1 and M2 goes through two stages; the first one is a rapid stage as soon as there is a strong adsorption until 61% for M1 and 46% for M2 in one hour; the second one is slow stage beyond 60 min the percentages can vary widely up to 240 min for M1 and M2. This is due to the availability of the high number of vacant adsorption sites on the surface of the two adsorbents at the initial stage of adsorption. However, the remaining unoccupied exterior sites are difficult to occupy due to the formation of repulsive forces between the effluent on the surface of the solid and those of the aqueous phase [32, 33]. These lead to a decrease in the adsorption rate, and a plateau is observed which corresponds to the state of equilibrium after 160 minutes.

To study the effect of adsorbents particles diameters, a series of experiments were performed with a constant adsorbent mass  $1.5\ \text{g}\cdot\text{L}^{-1}$ , dilution factor of 10, pH 10, and different mesh sizes of adsorbents particles at room temperature. Figure 7 illustrates that decreasing particles diameters ameliorate the adsorption percentage, and the  $40\ \mu\text{m}$  particle diameter has the highest adsorption rate 90% for M1 and 79% with M2. This could be explained by the relation between the active surface area of adsorbents materials and adsorption efficiency [34].

The pH is an important factor in any adsorption phenomenon, since it can influence both the adsorbent and adsorbate structures as well as the adsorption mechanism. The effect of the textile wastewater pH solution on the adsorption experiment using  $3\ \text{g}\cdot\text{L}^{-1}$  as dose of M1 or M2 and concentration dilution factor of 10 at room temperature was studied. The pH range of the solution was adjusted from 2 to 12 using HCl (0.5 M) and NaOH (0.5 M). It has been observed that adsorption percentage increases by rising the dye pH solution, where it reaches its maximum 93% and 86% for M1 and M2, respectively, at pH 10 (Figure 8). This behavior could be explained by the following: (i) at acidic pH,  $\text{H}^+$  ions will compete with dyes molecules, which reduce the adsorption efficiency. (ii) At basic pH, this competition decreases and the active sites become more negatively charged on M1 and M2 surface, which enhances the adsorption by electrostatic attraction forces [35]. In addition, we can conclude that the adsorbents' surfaces are negatively charged up to a pH 6.5 and 7.3 for M1 and M2, respectively, and positively charged below these values (Figure 9).

TABLE 2: Chemical composition of sieved clays (&lt;math&gt; &lt;80 \mu\text{m}&lt;/math&gt;) using XRF (%).

Samples	SiO <sub>2</sub>	Al <sub>2</sub> O <sub>3</sub>	Fe <sub>2</sub> O <sub>3</sub>	K <sub>2</sub> O	MgO	Na <sub>2</sub> O	CaO	TiO <sub>2</sub>	P <sub>2</sub> O <sub>5</sub>	LOI*
M1	53.6	26.5	5.61	2.1	2.05	1.5	0.67	0.84	0.18	6.58
M2	42.6	11	2.32	1.3	3.29	0.82	<b>18.8</b>	0.44	0.24	<b>18.7</b>

\*LOI: loss of ignition at 1000°C.

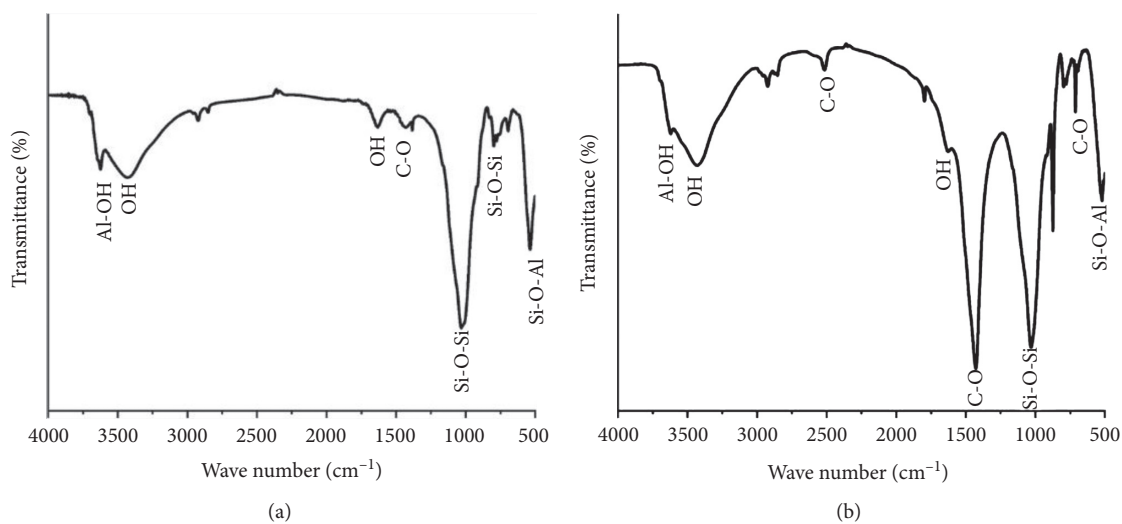


FIGURE 4: Infrared spectrum of both adsorbents.

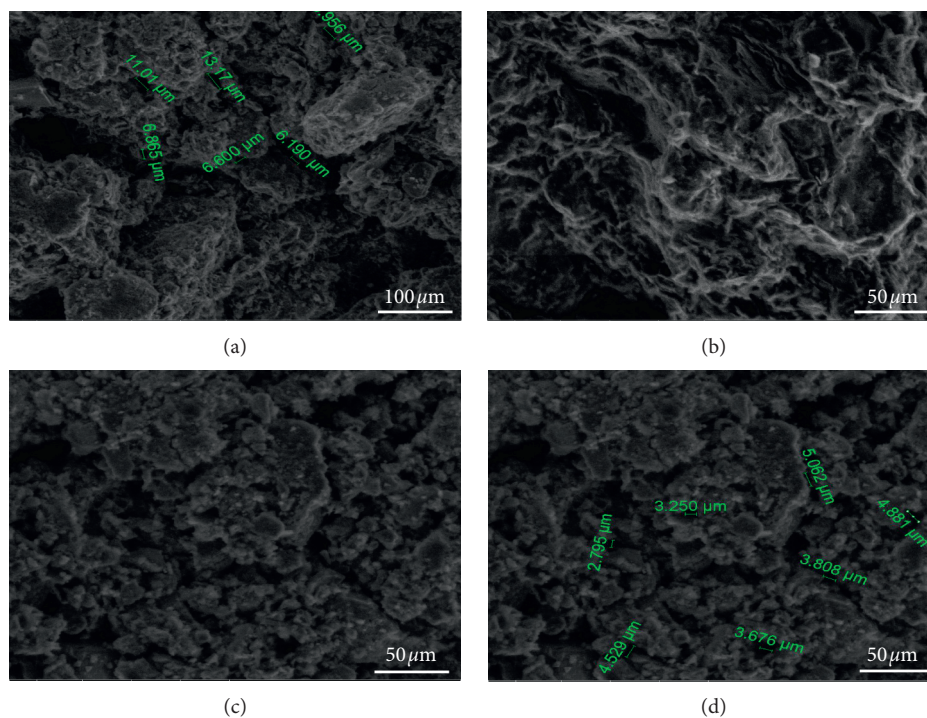


FIGURE 5: SEM images of M1 and M2 adsorbents.

The effect of textile wastewater concentration was studied over the adsorbents M1 and M2. A concentration dilution was varied in a range of 0–10 as a dilution factor using 1 g of adsorbents, pH 6 particle size 80  $\mu\text{m}$  at room

temperature. Figure 10 illustrates the adsorption evolution of textile wastewater over both adsorbents at different concentrations. The results revealed that adsorption efficiency decreases from 77 to 23% and from 64 to 14% with a

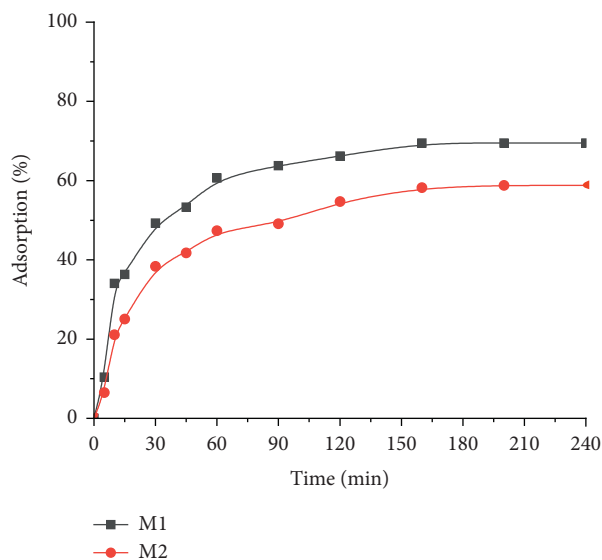


FIGURE 6: Time effect on the adsorption kinetic using M1 and M2.

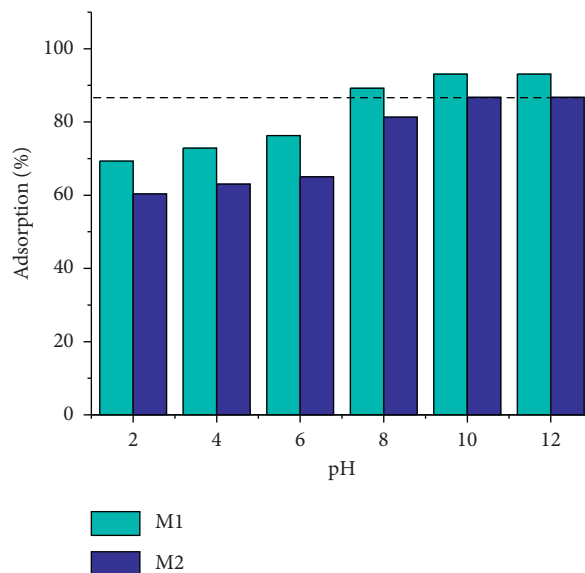


FIGURE 8: pH effect on wastewater textile dyes adsorption.

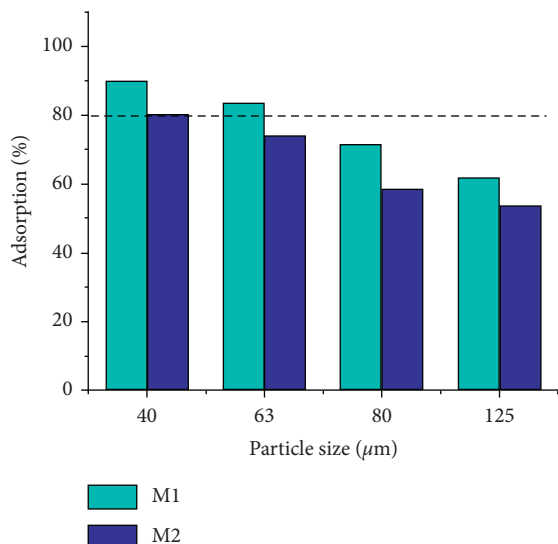
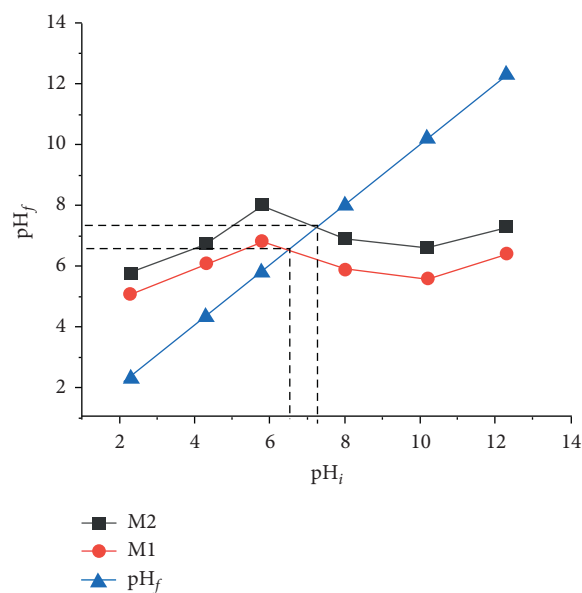


FIGURE 7: Adsorption percentage of textile dyes at different particle sizes.

decrease of concentration factor dilution from 10 to 0 for M1 and M2 adsorbents, respectively. This rate evolution could be explained by the low dispersion of pollutants' molecules into the adsorbents due to their high concentration. Furthermore, the high concentration of adsorbate saturates the adsorbents' active sites, which decreases the adsorption percentage [36].

The effects of M1 and M2 dosage on the adsorption of textile wastewater (pH 10, 40 μm, and 10 as dilution factor) were shown in Figure 11. The results indicate that the efficiency increased from 46 to 94% and from 30 to 86% when the adsorbents mass increased from 0.25 to 1.5 g·L<sup>-1</sup> for M1 and M2, respectively. These observations are in accordance with the increase of the active site on the adsorbents surface [37]. However, the wastewater concentration remains

FIGURE 9: pH<sub>pzc</sub> of the two raw adsorbents.

constant, whereas the adsorbents dose up to 2 g·L<sup>-1</sup> which means the saturation of the adsorbents surface.

Despite the fact that the effect of temperature on adsorption (pH 6, 80 μm, 1 g of adsorbent, and 10 as dilution factor) has been carefully studied using a sand bath to stabilize the temperature, no universal law has been found. Indeed, these studies have shown that an increase in temperature can lead to an increase in the adsorbed molecules amount. As shown in Figure 12 at higher temperature, the adsorbents lead to higher adsorption efficiency. As a result, enough energy ameliorates the adsorption fixation of pollutants molecules on the M1 and M2 active sites, that could be explained by the fact that the temperature creates new active sites capable of adsorbing more dyes molecules [38].

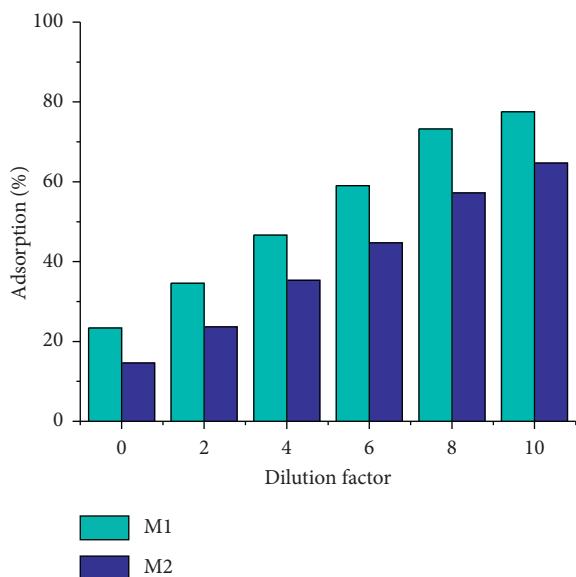


FIGURE 10: Adsorption of Essabbaghine textile on M1 and M2 at different dilutions.

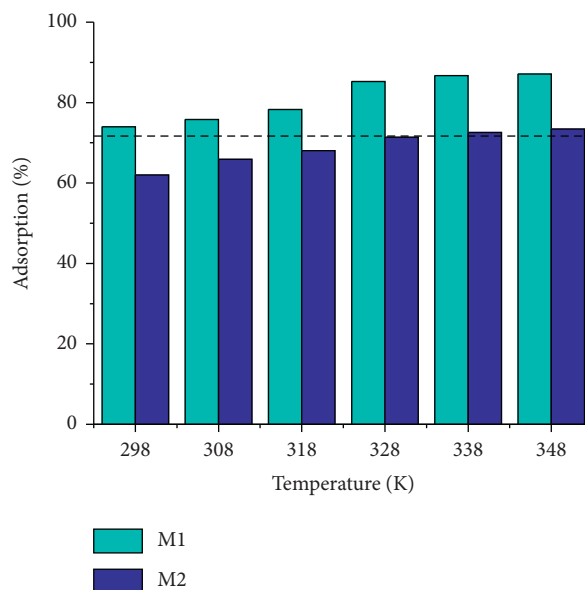


FIGURE 12: Temperature effect on adsorption evolution of textile dyes.

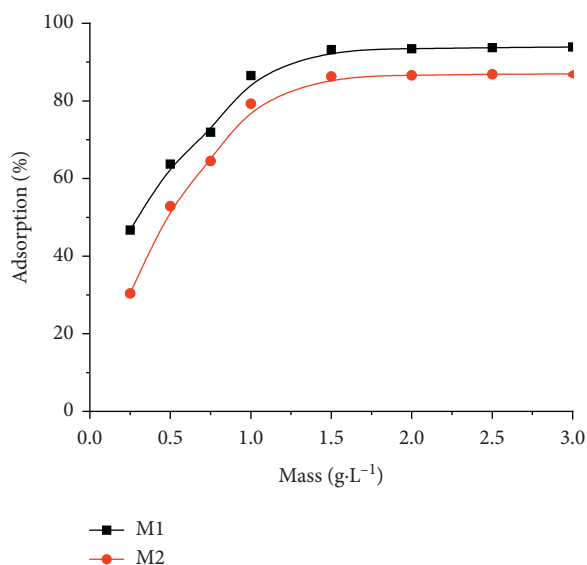


FIGURE 11: Mass adsorbent effect during the adsorption treatment.

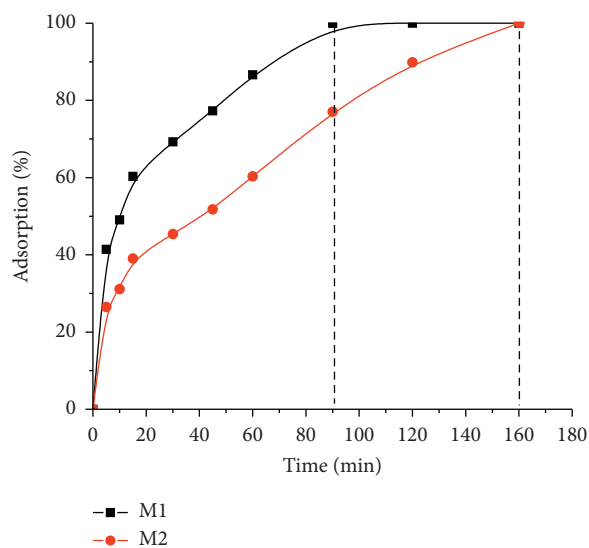


FIGURE 13: Adsorption under optimum conditions.

The adsorption treatment of textile dyes was tested through applying the optimal conditions found after it had been studied: adsorbent mass  $1.5 \text{ g}\cdot\text{L}^{-1}$ , 10 as dilution factor, 328 K in temperature,  $40 \mu\text{m}$  as particles diameters, pH 10, and the contact time of 90 and 160 minutes for M1 and M2, respectively. Figure 13 illustrates the evolution of the adsorption efficiency using M1 and M2 adsorbents. The adsorption percentage achieved 100% during 90 minutes for M1 and 160 minutes for M2.

It has been shown that textile wastewater was adequately treated at pH 10, which may be due to the formation of surface hydrogen bonds between the hydroxyl groups on both adsorbents' surface and the functional groups of textile

dyes as suggested in Figure 14. The large number of different functional groups on the adsorbents surface (e.g., carboxylic and hydroxyl groups) implied the existence of many types of adsorbent-adsorbate interactions. Moreover, the desorption studies show that adsorbed textile dyes onto M1 and M2 form a stable chemical bond between the adsorbents' surface and the pollutants' molecules, which prevented the dye molecules from being eluted from the adsorbents' surface using just water or heated water. However, small amounts of dyes molecules were eluted ( $\sim 20\%$ ) using NaCl and NaOH, and a high desorption was achieved with acidic agents. Figure 14 illustrates the electrostatic attraction between the dyes compound and adsorbents materials. This

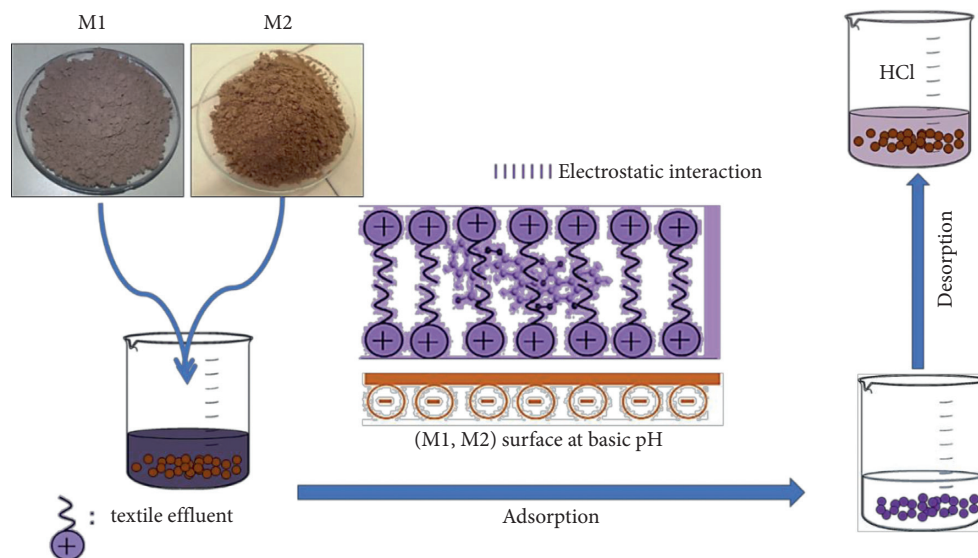


FIGURE 14: Adsorption procedure.

TABLE 3: Pseudo-first-order and pseudo-second-order parameters for adsorption of textile wastewater on both adsorbents surface M1 and M2.

Materials	$q_{\text{exp}}$ ( $\text{mg}\cdot\text{g}^{-1}$ )	$k_1$ ( $\text{min}^{-1}$ )	Pseudo-first-order		Pseudo-second-order		
			$q_e$ , calculated ( $\text{mg}\cdot\text{g}^{-1}$ )	$R^2$	$k_2$ ( $\text{g}\cdot\text{mg}^{-1}\cdot\text{min}^{-1}$ )	$q_e$ , calculated ( $\text{mg}\cdot\text{g}^{-1}$ )	$R^2$
M1	260	$6.64\cdot 10^{-2}$	347.8	0.872	$32\cdot 10^{-2}$	257.78	0.999
M2	245	$3.04\cdot 10^{-2}$	289.29	0.803	$83\cdot 10^{-2}$	241.26	0.997

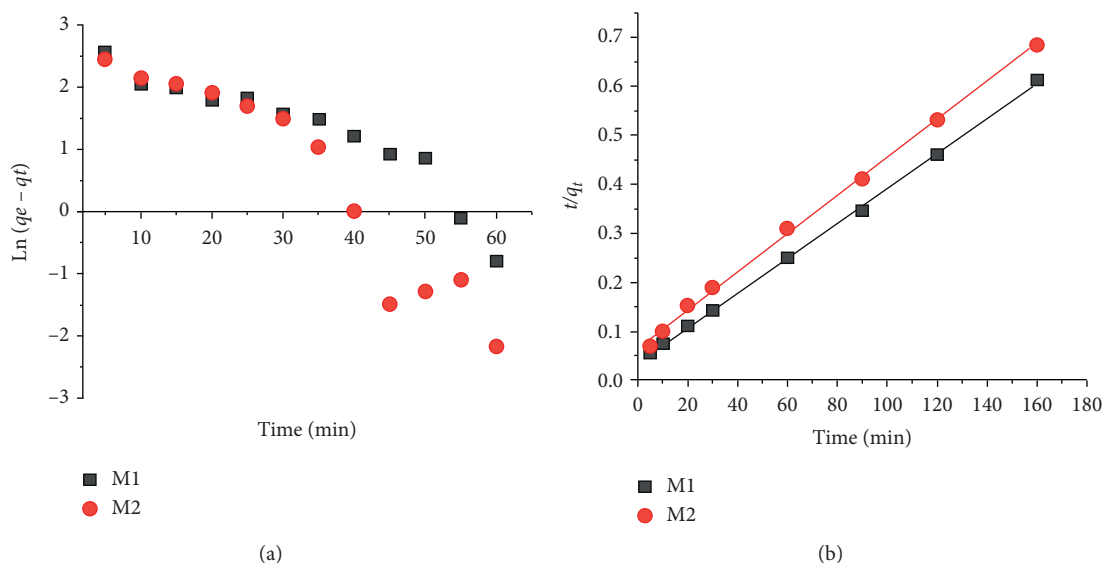


FIGURE 15: Pseudo-first-order and pseudo-second-order graphs of the adsorption.

phenomenon makes both materials suitable to adsorb more quantity of dye. At acidic condition, however, the presence of  $\text{H}^+$  will make dyes competing for ionic interact with the adsorbent [39].

**3.4. Kinetic Study.** The pseudo-first-order and pseudo-second-order for adsorption kinetics over M1 and M2 were evaluated. Table 3 and Figure 15 show that the values of the pseudo-first-order (PFO)  $R^2$  were 0.872 and 0.803, and the

values of the pseudo-second-order (PSO)  $R^2$  were 0.999 and 0.997 for M1 and M2, respectively; thus,  $R^2$  of the PSO was bigger than that of the (PFO), implying that the pseudo-second-order kinetic was the main kinetic process as long as it gives the best prediction for the kinetic data, and the adsorption capacity variable ( $q_e$ ) calculated is very close to the experimental capacity [16, 40].

Isotherm models (Langmuir and Freundlich) were studied to explain the adsorption system at equilibrium. All isotherms are executed with a variation of textile wastewater factory dilution 10. The results of adsorption isotherms show that the adsorption process of textile dyes onto M1 and M2 adsorbate fitted more strictly the isotherm Langmuir equation (4) than the Freundlich equation (5). This result is based on the higher value of  $R^2$ , which is considered as a measure of the excellent fit of experimental data on the isotherms models. The best isotherm that fits with both materials adsorptions is Langmuir. Thus, this process is a nonideal sorption on heterogeneous surfaces and multilayer sorption [16, 41]. The corresponding data of the two models are presented in Table 4.

### 3.5. Desorption Reaction and Adsorbents Regeneration.

Figure 16 reveals the effects of various chemical agents as eluents on the desorption efficiency. The desorption using 0.1 N HCl was optimum (89% for M1 and 78% for M2) followed by  $H_2SO_4$  (0.1 N),  $H_3PO_4$  (0.1 N), NaOH (0.1 N), and NaCl (0.1 N) [42]. The elution efficiency was further investigated at various HCl concentrations (Figure 16). This might be due to the deterioration of adsorption site on M1 and M2 surface in the presence of HCl agent.

The regeneration of both adsorbents is an important step in order to check the economic feasibility of the adsorption process. The regeneration studies were carried out using 0.1 N HCl solution as it gives optimum desorption elution (89.1%).

The regeneration studies were carried out in batch for five successive cycles using 200 mL of textile wastewater (Figure 17). Results showed that a decrease in the adsorption might be caused due to the decomposition by acidic solution to certain adsorption sites or functional groups present on M1 and M2 surface [33, 43].

### 3.6. Characteristics of the Treated Wastewater.

After the adsorption on the two natural materials, the treated textile wastewater was characterized to determine the performance of the treatment. Consequently, we paid particular attention to the dosages of heavy metals Cd, Cr, Cu, and Zn and of chemical oxygen demand (COD). The values obtained (Table 5) indicate an elimination of 88 and 79% of the COD for M1 and M2, respectively. In addition, the concentration of heavy metals decreases in the case of both materials. This achievement could be explained by the capacity of both materials to adsorb organic matter and metal ions present in the wastewater studied. The results summarized in Table 5 confirm that M1 is more efficient than M2.

TABLE 4: Adsorption isotherm constants for textile dyes adsorption onto the adsorbents.

Material	Langmuir isotherm parameters			Freundlich isotherm parameters		
	$q_m$ ( $mg \cdot g^{-1}$ )	$K_L$ ( $L \cdot g^{-1}$ )	$R^2$	$n$	$K_F$ ( $mg \cdot g^{-1}$ )	$R^2$
M1	321.43	0.173	0.994	3.303	27.04	0.606
M2	357.6	0.321	0.992	2.125	18.74	0.571

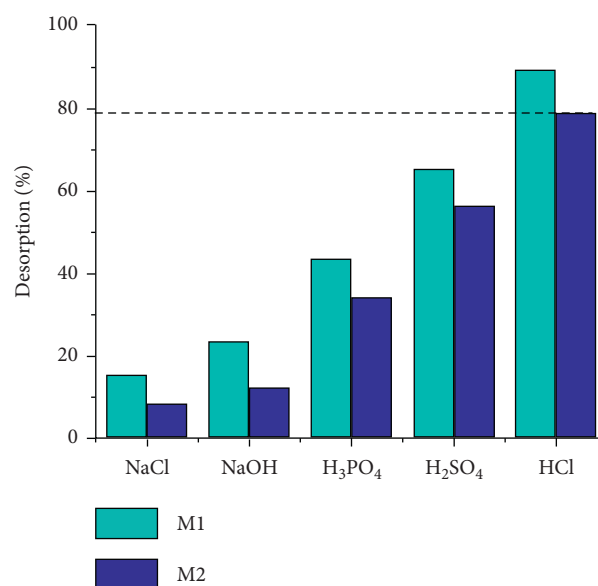


FIGURE 16: Desorption of textile dyes from M1 and M2 using various eluents.

### 3.7. Germination Test.

In this test, corn kernels were germinated with wastewater before and after adsorption in order to evaluate their toxicity and possible reuse. The results described in Table 6 make it possible to observe the effect of all samples (after and before adsorption treatment) on the germination rate of corn kernels compared to blank (potable water). 15 grains were used per experiment; they were arranged identically in Petri dishes and incubated in a culture chamber for 24 hours. 5 ml of each solution (water, S1, and S2) was added which corresponds to  $T_0$  of imbibition then 5 ml of each solution was added every 24 hours of incubation at  $13^\circ C$  for 6 days. The percentage of germination is noted every 24 hours. Figure 18 shows that in 6 days the germination of corn kernels using distilled water was successfully done. Moreover, the germination rate using treated effluent (S1) with both M1 and M2 materials achieved 97.8% in 6 days, which confirm a good adsorption yield. Unlike untreated solutions, the germination rate does not exceed 20%. As the toxicity depends on the concentration of pollutants in the solutions, the germination increases at low pollutants concentration [21, 44]. These results confirm the possibility of reusing the treated textile wastewater to irrigate plants in urban gardens.

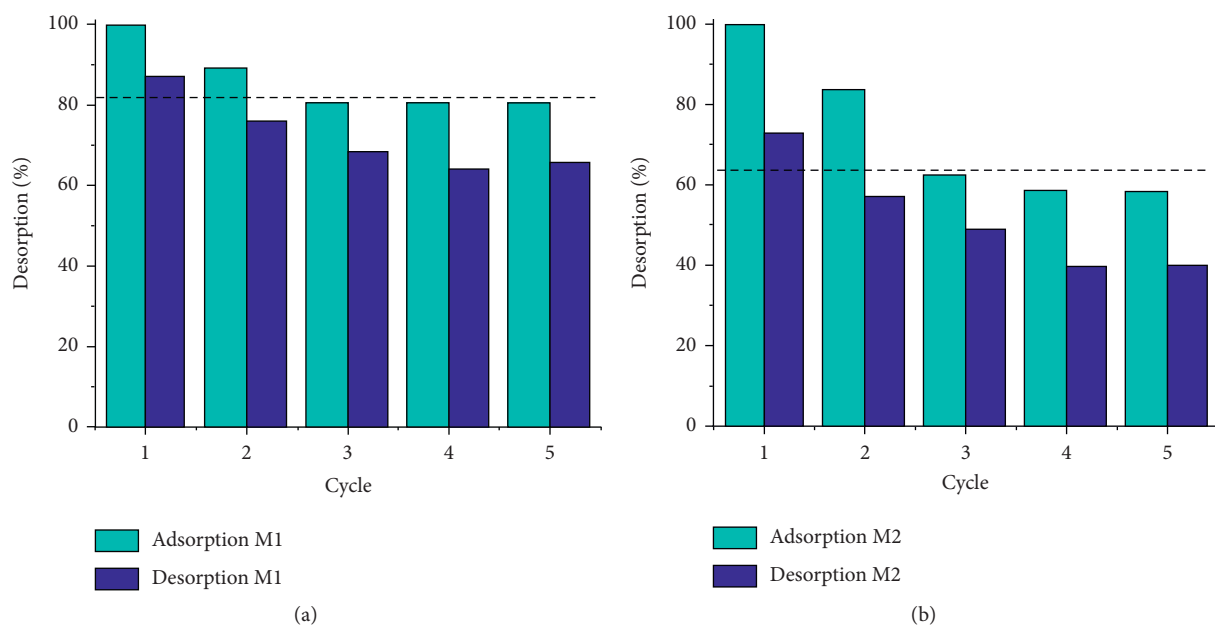


FIGURE 17: Regeneration studies of M1 (a) and M2 (b).

TABLE 5: Comparison of wastewater parameters before and after treatment.

Parameters	Wastewater before treatment	Wastewater after treatment		Elimination percentage (%)	
		M1	M2	M1	M2
COD (mg O <sub>2</sub> ·L <sup>-1</sup> )	440	49.8	89.16	88.68	79.73
Cd (mg·L <sup>-1</sup> )	0.0484	0.031	0.039	35.95	19.42
Cr (mg·L <sup>-1</sup> )	0.2469	0.1499	0.188	39.43	23.57
Cu (mg·L <sup>-1</sup> )	0.1451	0.1041	0.1189	28.27	18.62
Zn (mg·L <sup>-1</sup> )	1.2963	0.78	0.9894	39.53	24.03

TABLE 6: Number of germinated corn kernels and germination rate (three replicates for each study).

	Number of germinated corn kernels	Germination rate (%)
Blank	15/15/15	100
After adsorption (S1)	14/15/15	97.78
Before adsorption (S2)	3/3/3	20

#### 4. Performance Comparison with Literature

The efficiency of the adsorption towards different dyes effluents according to literature studies is presented in Table 7 [8, 18, 45–48] in which we have involved the results of the present work as well as the necessary conditions to establish comparisons. Table 7 confirms that the present work shows an important adsorption of dyes during two hours. Consequently, Moroccan materials could be a promising adsorbent for the elimination of dyes. However, it was evident from the studies of textile wastewater adsorption, that it would be interesting and it is currently in progress in our lab to activate those materials which can be a promising material for wastewater treatment

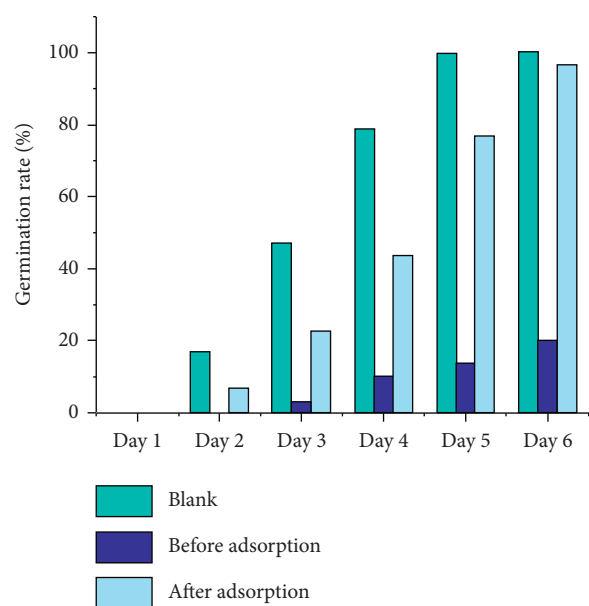


FIGURE 18: Variation of germination rate of corn kernels during 6 days.

TABLE 7: Comparison of the treatment efficiency with literature studies.

Adsorbent	Real rejection	Adsorption (%)	Reference
Clay from the Fouchana region (Tunisia)	Dyeing industry	(i) 97.0% BOD <sub>5</sub> (ii) 95.0% COD	[8]
Powder (a-NLP)	Textile effluent	(i) 98.9% BOD <sub>5</sub> (ii) 100% COD	[45]
Activated charcoal	Textile effluent	(i) 81.0% BOD <sub>5</sub> (ii) 87.6% COD	[46]
(i) Alum (ii) Activated carbon (iii) Alum + activated carbon	Textile effluent	92% COD	[47]
Graphene oxide (GO)	Textile effluent	85.0% turbidity 60.0% color in 30 min	[18]
Synthetic compounds based on iron/aluminum	Dyeing polyester fabric at acid pH	(i) 60.0% COD	[48]
Natural material (M1 and M2)	Textile effluent	(i) M1:88% COD (ii) M2:79% COD	Present work

## 5. Conclusion

In this study, the ability of using both natural materials M1 from Tiflet and M2 from Berrechid areas as adsorbents has been explored. Without pretreatment or activation, both materials have been used and proved effectiveness to remove dyes from real textile wastewater samples of Fez city. In addition to the advantage of their availability in large quantities, they present an eco-friendly alternative to traditional processes of wastewater treatment, even though the test of adsorption–desorption cycles demonstrates that both of them cannot be used several times, they are still cost-effective adsorbents, taking into account the high adsorption yield reached. Another advantage of using these two materials is the possibility of removing different types of organic compounds and heavy metals having an attractive potential on the surface of the adsorbents. It would be interesting to continue testing on real wastewater not only batch processes but also column processes in pilot scale.

## Data Availability

The authors confirm that all data underlying the findings of this study are fully available without restriction.

## Conflicts of Interest

The authors declare that they have no conflicts of interest regarding the publication of this paper.

## Acknowledgments

The authors thank the general services (DRX, FTIR, SEM, etc.) of the Innovation Center of the University of Fez (Morocco).

## References

- [1] A. Aleboyeh, H. Aleboyeh, and Y. Moussa, “Decolorisation of acid blue 74 by ultraviolet/H<sub>2</sub>O<sub>2</sub>,” *Environmental Chemistry Letters*, vol. 1, no. 3, pp. 161–164, 2003.
- [2] S. Peker, S. Yapar, and N. Beşün, “Adsorption behavior of a cationic surfactant on montmorillonite,” *Colloids and Surfaces A: Physicochemical and Engineering Aspects*, vol. 104, no. 2-3, pp. 249–257, 1995.
- [3] N. D. Lourenço, J. M. Novais, and H. M. Pinheiro, “Reactive textile dye colour removal in a sequencing batch reactor,” *Water Science & Technology*, vol. 42, pp. 321–328, 2018.
- [4] S. Liu, Y. Ding, P. Li et al., “Adsorption of the anionic dye Congo red from aqueous solution onto natural zeolites modified with N,N-dimethyl dehydroabietylamine oxide,” *Chemical Engineering Journal*, vol. 248, pp. 135–144, 2014.
- [5] S. Sen and G. N. Demirer, “Anaerobic treatment of real textile wastewater with a fluidized bed reactor,” *Water Research*, vol. 37, pp. 1868–1878, 2003.
- [6] K. P. Sharma, S. Sharma, S. Sharma et al., “A comparative study on characterization of textile wastewaters (untreated and treated) toxicity by chemical and biological tests,” *Chemosphere*, vol. 69, no. 1, pp. 48–54, 2007.
- [7] Z.-Y. Yao, J.-H. Qi, and L.-H. Wang, “Equilibrium, kinetic and thermodynamic studies on the biosorption of Cu(II) onto chestnut shell,” *Journal of Hazardous Materials*, vol. 174, no. 1–3, pp. 137–143, 2010.
- [8] E. Errais, J. Duplay, and F. Darragi, “Textile dye removal by natural clay—case study of fouchana Tunisian clay,” *Environmental Technology*, vol. 31, no. 4, pp. 373–380, 2010.
- [9] J.-W. Lee, S.-P. Choi, R. Thiruvenkatachari, W.-G. Shim, and H. Moon, “Evaluation of the performance of adsorption and coagulation processes for the maximum removal of reactive dyes,” *Dyes and Pigments*, vol. 69, no. 3, pp. 196–203, 2006.
- [10] E. GilPavas, I. Dobrosz-Gómez, and M. Á. Gómez-García, “Coagulation-flocculation sequential with fenton or photo-fenton processes as an alternative for the industrial textile wastewater treatment,” *Journal of Environmental Management*, vol. 191, pp. 189–197, 2017.
- [11] M. Punzi, F. Nilsson, A. Anbalagan et al., “Combined anaerobic-ozonation process for treatment of textile wastewater: removal of acute toxicity and mutagenicity,” *Journal of Hazardous Materials*, vol. 292, pp. 52–60, 2015.
- [12] K. Tanji, J. A. Navio, A. N. Martín-Gómez et al., “Role of Fe(III) in aqueous solution or deposited on ZnO surface in the photoassisted degradation of rhodamine B and caffeine,” *Chemosphere*, vol. 241, Article ID 125009, 2019.
- [13] K. Tanji, J. A. Navio, J. Naja et al., “Extraordinary visible photocatalytic activity of a Co<sub>0.2</sub>Zn<sub>0.8</sub>O system studied in the remazol BB oxidation,” *Journal of Photochemistry and Photobiology A: Chemistry*, vol. 382, p. 111877, 2019.
- [14] M. Zouhier, K. Tanji, J. A. Navio, M. C. Hidalgo, C. Jaramillo-Páez, and A. Kherbeche, “Preparation of ZnFe<sub>2</sub>O<sub>4</sub>/ZnO

- composite: effect of operational parameters for photocatalytic degradation of dyes under UV and visible illumination," *Journal of Photochemistry and Photobiology A: Chemistry*, vol. 390, Article ID 112305, 2020.
- [15] M. C. Ncibi, B. Mahjoub, and M. Seffen, "Adsorptive removal of textile reactive dye using *Posidonia oceanica* (L.) fibrous biomass," *International Journal of Environmental Science & Technology*, vol. 4, no. 4, pp. 433–440, 2007.
- [16] M. Kachabi, I. El Mrabet, Z. Benchekroun, M. Nawdali, and Z. Hicham, "Synthesis and adsorption properties of activated carbon from KOH-activation of Moroccan Jujube shells for the removal of COD and color from wastewater," *Mediterranean Journal of Chemistry*, vol. 8, no. 3, pp. 168–178, 2019.
- [17] F. Mejbar, Y. Miyah, A. El Badraoui et al., "Studies of the adsorption kinetics process for removal of methylene blue dye by residue of grenadine bark extraction," *Moroccan Journal of Chemistry*, vol. 6, pp. 436–443, 2019.
- [18] C. M. Bezerra de Araujo, G. Filipe Oliveira do Nascimento, G. Rodrigues Bezerra da Costa et al., "Adsorptive removal of dye from real textile wastewater using graphene oxide produced via modifications of Hummers method," *Chemical Engineering Communications*, vol. 206, pp. 1–13, 2018.
- [19] M. S. Larrechi, M. P. Callao, and V. Gomez, "Kinetic and adsorption study of acid dye removal using activated carbon," *Chemosphere*, vol. 69, pp. 1151–1158, 2007.
- [20] N. Loubna, Y. Miyah, O. Assila, A. El Badraoui, B. El Khazzan, and F. Zerrouq, "Kinetic and thermodynamic study of the adsorption of two dyes: brilliant green and eriochrome black T using a natural adsorbent "sugarcane bagasse"" *Moroccan Journal of Chemistry*, vol. 7, pp. 715–726, 2019.
- [21] B. Sancey, *Développement de la Bio-Adsorption pour Décontaminer des Effluents de Rejets Industriels: Abattement Chimique et Gain Environnemental*, Université de Franche-Comté, Besançon, France, 2014.
- [22] B. Sancey, G. Trunfio, J. Charles et al., "Heavy metal removal from industrial effluents by sorption on cross-linked starch: chemical study and impact on water toxicity," *Journal of Environmental Management*, vol. 92, no. 3, pp. 765–772, 2011.
- [23] Bulletin Officiel, *Les Normes Marocaines des Rejets Liquides dans les Eaux de Surface et Souterraine*, Bulletin Officiel, 2018.
- [24] H. Çelik, "Technological characterization and comparison of two ceramic clays used for manufacturing of traditional ceramic products in Turkey," *Mining*, vol. 56, pp. 137–147, 2017.
- [25] D. Feng, X. Li, X. Wang et al., "Water adsorption and its impact on the pore structure characteristics of shale clay," *Applied Clay Science*, vol. 155, pp. 126–138, 2018.
- [26] L. D. Youcef, L. S. Belaroui, and A. López-Galindo, "Adsorption of a cationic methylene blue dye on an Algerian palygorskite," *Applied Clay Science*, vol. 179, Article ID 105145, 2019.
- [27] N. Chaudhary and C. Balomajumder, "Optimization study of adsorption parameters for removal of phenol on aluminum impregnated fly ash using response surface methodology," *Journal of the Taiwan Institute of Chemical Engineers*, vol. 45, no. 3, pp. 852–859, 2014.
- [28] S. Velu, L. Wang, M. Okazaki, K. Suzuki, and S. Tomura, "Characterization of MCM-41 mesoporous molecular sieves containing copper and zinc and their catalytic performance in the selective oxidation of alcohols to aldehydes," *Microporous and Mesoporous Materials*, vol. 54, no. 1–2, pp. 113–126, 2002.
- [29] S. Mohammadnejad, J. L. Provis, and J. S. J. van Deventer, "Effects of grinding on the preg-robbing behaviour of pyrophyllite," *Hydrometallurgy*, vol. 146, pp. 154–163, 2014.
- [30] A. El Gaidoumi, A. Chaouni Benabdallah, A. Lahrichi, and A. Kherbeche, "Adsorption of phenol in aqueous medium by raw and treated moroccan pyrophyllite," *Journal of Materials and Environmental Science*, vol. 6, pp. 2247–2259, 2015.
- [31] T. B. Musso, M. E. Parolo, G. Pettinari, and F. M. Francisca, "Cu(II) and Zn(II) adsorption capacity of three different clay liner materials," *Journal of Environmental Management*, vol. 146, pp. 50–58, 2014.
- [32] M.-S. Chiou and H.-Y. Li, "Equilibrium and kinetic modeling of adsorption of reactive dye on cross-linked chitosan beads," *Journal of Hazardous Materials*, vol. 93, no. 2, pp. 233–248, 2002.
- [33] M. R. Malekbala, M. A. Khan, S. Hosseini, L. C. Abdullah, and T. S. Y. Choong, "Adsorption/desorption of cationic dye on surfactant modified mesoporous carbon coated monolith: equilibrium, kinetic and thermodynamic studies," *Journal of Industrial and Engineering Chemistry*, vol. 21, pp. 369–377, 2015.
- [34] L.-F. Chen, H.-H. Wang, K.-Y. Lin, J.-Y. Kuo, M.-K. Wang, and C.-C. Liu, "Removal of methylene blue from aqueous solution using sediment obtained from a canal in an industrial park," *Water Science and Technology*, vol. 78, no. 3, pp. 556–570, 2018.
- [35] D.-S. Kim, "Short communication: measurement of point of zero charge of bentonite by solubilization technique and its dependence of surface potential on pH," *Environmental Engineering Research*, vol. 8, no. 4, pp. 222–227, 2003.
- [36] H. B. Hadjltaief, S. B. Ameer, P. Da Costa, M. B. Zina, and M. E. Galvez, "Photocatalytic decolorization of cationic and anionic dyes over ZnO nanoparticle immobilized on natural Tunisian clay," *Applied Clay Science*, vol. 152, pp. 148–157, 2018.
- [37] M. A. Khalque, S. S. Ahammed, S. A. Khan, K. A. Rabbani, M. E. Islam, and M. S. Alam, "Reactive dye removal from industrial wastewater on cotton dust as a bio adsorbent," *International Journal of Scientific & Technology Research*, vol. 7, pp. 45–48, 2018.
- [38] A. B. Karim, B. Mounir, M. Hachkar, M. Bakasse, and A. Yaacoubi, "Élimination du colorant basique "bleu de méthylène" en solution aqueuse par l'argile de Safi," *Journal of Water Sciences*, vol. 23, no. 4, pp. 375–388, 2010.
- [39] R. Hachani, H. Sabir, N. Sana, K. F. Zohra, and N. M. Nesrine, "Performance study of a low-cost adsorbent-raw date pits-for removal of azo dye in aqueous solution," *Water Environment Research*, vol. 89, no. 9, pp. 827–839, 2017.
- [40] M. A. Al-ghouti, J. Li, Y. Salamh, N. Al-laqtah, G. Walker, and M. N. M. Ahmad, "Adsorption mechanisms of removing heavy metals and dyes from aqueous solution using date pits solid adsorbent," *Journal of Hazardous Materials*, vol. 176, no. 1–3, pp. 510–520, 2010.
- [41] Z. Benchekroun, I. El Mrabet, M. Kachabi, M. Nawdali, I. Neves, and H. Zaitan, "Removal of basic dyes from aqueous solutions by adsorption onto Moroccan clay (Fez city)," *Mediterranean Journal of Chemistry*, vol. 8, pp. 158–167, 2019.
- [42] Z. Chaouki, K. Fouad, M. Ijjaali et al., "Use of combination of coagulation and adsorption process for the landfill leachate treatment from Casablanca city," *Desalination and Water Treatment*, vol. 83, pp. 262–271, 2017.
- [43] A. É. D. Khalfaoui, "Étude expérimentale de l'élimination de polluants organiques et inorganiques par adsorption sur des matériaux naturels: application aux peaux d'orange et de banane," 2012, [https://bu.umc.edu.dz/md/index.php?lvl=notice\\_display&id=6134](https://bu.umc.edu.dz/md/index.php?lvl=notice_display&id=6134).

- [44] F. Anzala, "Contrôle de la vitesse de germination chez le maïs (*Zea mays*): étude de la voie de biosynthèse des acides aminés issus de l'aspartate et recherche de QTLs," 2007, <https://tel.archives-ouvertes.fr/tel-00181021>.
- [45] H. Patel and R. T. Vashi, "Batch adsorption treatment of textile wastewater," *Characterization and Treatment of Textile Wastewater*, pp. 111–125, 2015.
- [46] H. Patel and R. T. Vashi, "Treatment of textile wastewater by adsorption and coagulation," *E-Journal of Chemistry*, vol. 7, no. 4, pp. 1468–1476, 2010.
- [47] M. Aleem, J. Cao, C. Li et al., "Coagulation- and adsorption-based environmental impact assessment and textile effluent treatment," *Water, Air, & Soil Pollution*, vol. 45, p. 231, 2020.
- [48] F. Zidane, A. Rhazzar, J.-F. Blais et al., "Contribution à la dépollution des eaux usées de textile par électrocoagulation et par adsorption sur des composés à base de fer et d'aluminium," *International Journal of Biological and Chemical Sciences*, vol. 5, pp. 1727–1745, 2011.